

Proceedings of the 2nd Winter Workshop S&amp;SRES'96, Polanica Zdrój 1996

# ELECTRON SPIN RESONANCE STUDY OF $\text{Nd}^{3+}$ AND $\text{Er}^{3+}$ IONS IN $\text{YAIO}_3$

R. JABŁOŃSKI AND Z. FRUKACZ

Institute of Electronic Materials Technology  
133 Wólczyńska, 01-919 Warsaw, Poland

In this paper we present the results of ESR and photo-ESR measurements on  $\text{YAIO}_3(\text{YAP})$  single crystals and powder samples doped purposely with about 1 at.%  $\text{Nd}^{3+}$  and undoped crystals in which  $\text{Er}^{3+}$  was observed as residual dopant. The ESR measurements were carried out at X-band spectrometer in 4–300 K temperature range. The photo-ESR was performed at 5 K using a mercury arc lamp. For the  $\text{Nd}^{3+}$  doped crystals the intensity of ESR signal decreased about 2 times during illumination conditions. Moreover, the calculations of the  $g$  tensor and  $A$  hyperfine structure parameters for  $\text{Nd}^{3+}$  and  $\text{Er}^{3+}$  were carried out.

PACS numbers: 76.30.-v, 61.72.-y, 42.70.Hj

## 1. Introductions

Yttrium aluminum perovskite  $\text{YAIO}_3$  (YAP) is a host crystal which supports laser action when containing rare-earth ions and transition-metal ions. The ESR spectra of transition-metal ions such as  $\text{Cr}^{3+}$ ,  $\text{Fe}^{3+}$  and  $\text{Tl}^{3+}$  in YAP were carried out at room temperature and 1.6 K [1–3]. Up to now, there are no papers dealing with ESR investigation of  $\text{Nd}^{3+}$  and  $\text{Er}^{3+}$  doped YAP crystals. In contrast, the relaxation processes in the formation and decay of defect centers were studied by ESR and photoinduced ESR in a number of laser oxide crystals such as YAP and YAG doped  $\text{Cr}^{3+}$ ,  $\text{Fe}^{3+}$  [4–6]. This paper demonstrates the relationship between the intensity of the ESR signal as a function of the illumination with ultraviolet light in the crystals doped with 2%  $\text{Nd}^{3+}$ .

## 2. Experimental procedure

Single crystals were grown by Czochralski method from the melt containing 2 mol%  $\text{Nd}_2\text{O}_3$ . In pure single crystal  $\text{Er}^{3+}$  was observed as residual dopant. Samples with dimensions  $3.5 \times 3.5 \times 5 \text{ mm}^3$  were cut from boules, the cut faces being normal to the [100], [010], and [001] directions associated with the  $a$ ,  $b$  and  $c$  axes of the crystal. The ESR experiments were performed with BRUKER ESP 300 spectrometer working at X-band (9.4 GHz) in the range from 4 K to 70 K. The sample was rotated using a goniometer in a rectangular optical transmission X-band cavity type ER 4104 OR operating in the  $\text{TE}_{103}$  mode.

### 3. ESR measurements

#### 3.1. YAP:Nd<sup>3+</sup>

The ESR spectra were measured at X-band ( $\nu = 9.43$  GHz) at 15 K. Figure 1 shows the typical X-band ESR spectra consisting of a single resonance line with several weak satellite lines, associated with the hyperfine structure due to the nuclear spin of isotopes  $^{143}\text{Nd}^{3+}$  ( $I = 7/2$ ) and  $^{145}\text{Nd}^{3+}$  ( $I = 7/2$ ) with natural abundances of 12.2% and 8.3%, respectively. The inset shows the time dependence

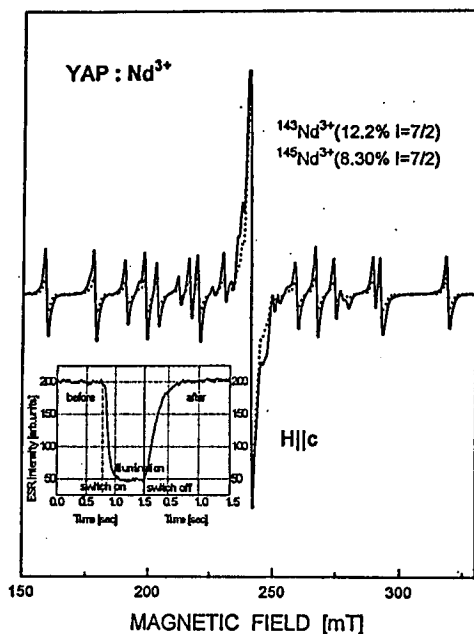


Fig. 1. The YAP:Nd<sup>3+</sup> ESR spectrum at 5 K, the satellite lines are the hyperfine transitions corresponding to the nuclear isotopes 143 and 145, respectively. The inset shows the time dependence of the intensity of the ESR signal after switching on or switching off UV illumination.

of the ESR signal intensity after switching on or switching off the UV illumination. The photo-ESR was performed at 5 K,  $P = 0.2$  mW, using mercury arc lamp. Figure 2 shows the angular dependence of the ESR spectra as the magnetic field is rotated in the  $a$ - $b$  plane. The ESR spectra at some magnetic field directions consist of two resonance lines. The two lines converge to a single line when the applied magnetic field is parallel to the  $a$ ,  $b$  and  $c$  direction. These results indicate that the ESR signals are due to two inequivalent sites which become equivalent when the magnetic field is parallel to the  $a$ ,  $b$  and  $c$  axes. The angular dependence of the ESR spectra are fitted by the spin Hamiltonian

$$\mathcal{H} = \beta \mathbf{H} \cdot \mathbf{g} \cdot \mathbf{S} + \mathbf{S} \cdot \mathbf{A} \cdot \mathbf{I},$$

$$g^2 A^2 = l^2 g_x^2 A_x^2 + m^2 g_y^2 A_y^2 + n^2 g_z^2 A_z^2, \quad (1)$$

where  $S = 1/2$ , and  $\beta$  is the Bohr magneton,  $A$  is the hyperfine structure constant,  $g$  — Lande factor [7]. The principle axis  $z$  lies in the  $a$ - $b$  plane and creates  $\theta$  angle with  $a$ -axis. The full curves in Fig. 2 were calculated using Eq. (1) with the spin-Hamiltonian parameters and the  $\theta_z$  polar angles listed in Table. The peak-to-peak intensities of the ESR signals decrease with increasing temperature and are not detected above 50 K because of line broadening. Figure 3 shows typical spectrum for a powder sample.

TABLE

Spin-Hamiltonian parameters and polar angles.

	$g_x$	$g_y$	$g_z$	$A_x$ [ $10^{-4}$ cm $^{-1}$ ]	$A_y$ [ $10^{-4}$ cm $^{-1}$ ]	$A_z$ [ $10^{-4}$ cm $^{-1}$ ]	$\theta_z$ [deg]
$^{143}\text{Nd}^{3+}$	2.812(5)	2.554(5)	1.700(2)	212.6(5)	217.9(5)	206.3(5)	27.76
$^{145}\text{Nd}^{3+}$	"	"	"	131.7(5)	103.7(5)	147.1(5)	"
$^{167}\text{Er}^{3+}$	8.954(5)	8.128(5)	2.787(2)	70.0(5)	74.2(5)	167.8(5)	41.54

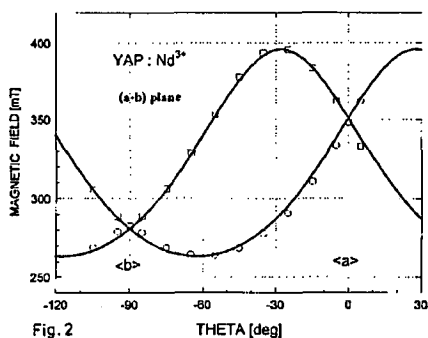


Fig. 2

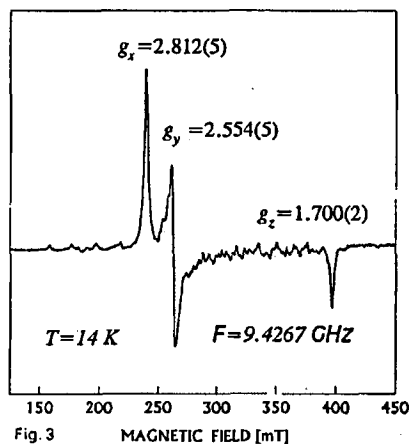


Fig. 3

Fig. 2. Angular dependence of the ESR spectra of  $\text{YAP:Nd}^{3+}$  at 15 K with the magnetic field in the  $a$ - $b$  plane. The solid line was calculated using Eq. (1) and the spin-Hamiltonian parameters in Table.

Fig. 3. Derivative presentation of the ESR spectrum polycrystalline (powder)  $\text{YAP:Nd}^{3+}$  with three principal  $g$  values..

### 3.2. $\text{YAP:Er}^{3+}$

The ESR spectra of  $\text{Er}^{3+}$  doped crystals for  $H \parallel c$ -axis is depicted in Fig. 4. It consists of a single resonance line with several weak satellite lines, associated with hyperfine structure due to the nuclear spin of the  $^{167}\text{Er}^{3+}$  ( $I = 7/2$ ) isotope with natural abundance of 22.9%. The angular dependence of the ESR spectra when the magnetic field is rotated in the  $a$ - $b$  plane is presented in Fig. 5. It shows

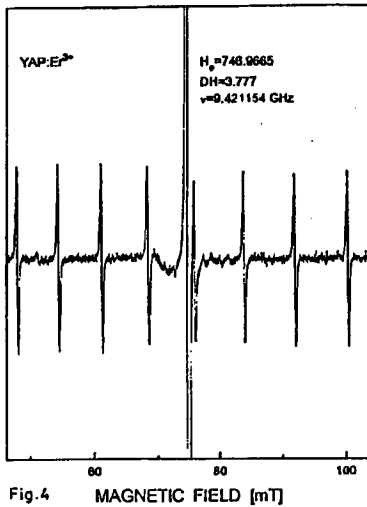


Fig.4

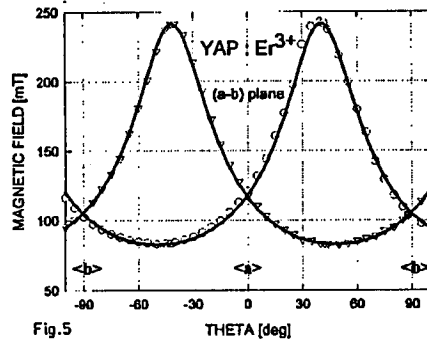


Fig.5

Fig. 4. The YAP:Er<sup>3+</sup> ESR spectrum at 15 K with the magnetic field applied parallel to the *c*-axis direction, the satellite lines are the hyperfine transitions corresponding to <sup>167</sup>Er isotope with natural abundances 22.9% and nuclear spin  $I = 7/2$ .

Fig. 5. Angular dependence of the ESR spectra of YAP:Er<sup>3+</sup> at 15 K with the magnetic field in the *a*-*b* plane. The solid line was calculated using Eq. (1) and the spin-Hamiltonian parameters in Table.

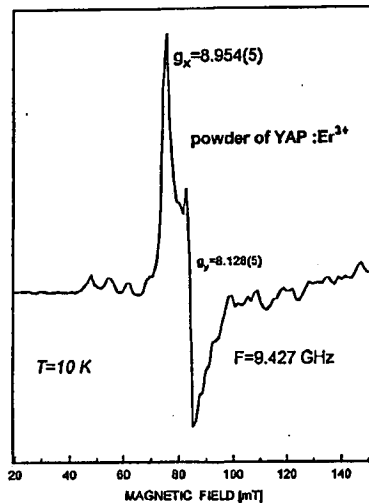


Fig. 6. Derivative presentation of the ESR spectrum polycrystalline (powder) YAP:Er<sup>3+</sup> with two principal *g* values.

similar behavior as in Nd<sup>3+</sup>doped crystals. This means that for some magnetic field directions, two resonance lines are observed. Figure 6 shows spectrum typical of a powder sample. The ESR signals are not detected above 50 K.

#### 4. Conclusions

YAP has a slightly distorted perovskite structure with orthorhombic symmetry. The rare-earth sites are coupled in pairs by an inversion through the aluminum sites, so there are only two magnetically inequivalent rare-earth sites for any orientation of  $H$ . For  $H$  in the  $b$ - $c$  or  $a$ - $c$  planes the four sites are all magnetically equivalent. The anisotropy of the crystal structure was measured by the ESR absorption spectra of  $Nd^{3+}$  and  $Er^{3+}$  ions replacing  $Y^{3+}$  in dodecahedral sites. The principal axes of the  $Nd^{3+}$  and  $Er^{3+}$  complexes determined by the ESR measurement are  $\theta_z = 27.76^\circ$  and  $41.54^\circ$ , respectively. This set of axes indicates severe local distortions at the rare-earth site. The values of  $g$  factors can be estimated from the degree of the orthorhombic distortion, because they are determined by the spin-orbit coupling. In agreement with Abragam calculations [7] we can fit the observed values for the ground state, and we can test the accuracy of the fit for  $Nd^{3+}$  by calculating the value of the quantity

$$9g_{\perp}^2/4/(g_{\parallel} + 5\Lambda)/(7\Lambda - g_{\parallel}) = 1,$$

where  $\Lambda = 8/11$  and assuming that  $g_{\perp} = (g_x + g_y)/2$ , and  $g_{\parallel} = g_z$ . Using our experimental  $g$ -values we obtain the value of 0.96. Similarly for  $Er^{3+}$

$$[(g_{\parallel} - \Lambda)/6\Lambda]^2 + 1/55(g_{\perp}/\Lambda)^2 = 1,$$

where  $\Lambda = 6/5$ , we obtained the value of 0.907. Our results show that in both cases we obtained good approximation to the ground state.

#### References

- [1] M. Yamaga, H. Tekeuchi, T.P.J. Han, B. Henderson, *J. Phys., Condens. Matter* **5**, 8097 (1993).
- [2] R.L. White, G.F. Herrmann, J.W. Carson, M. Mandel, *Phys. Rev.* **136**, A231 (1964).
- [3] M. Yamaga, T. Yosida, B. Henderson, K.P. O'Donnell, M. Date, *J. Phys., Condens. Matter* **4**, 7285 (1992).
- [4] O.F. Schrrimer, K.W. Blazey, W. Berlinger, R. Diechl, *Phys. Rev. B* **11**, 4201 (1975).
- [5] W.A. Akerman, G.R. Bulka, D.I. Wainstein, W.M. Winkurov, W.W. Winkurova, A.A. Galeev, W.M. Garmasz, G.A. Jermakov, A.A. Markelov, N.M. Nizamutdinov, N.II. Hasanova, *Fiz. Tverd. Tela* **31**, 214 (1989).
- [6] D.I. Vainsthein, *Radiat. Eff. Solids* **119-121**, 533 (1991).
- [7] A. Abragam, B. Bleaney, *Electron Paramagnetic Resonance of Transition Ions*, Clarendon Press, Oxford 1970, p. 167, 313, 320.